Am J Transl Res 2025;17(11):8712-8723
www.ajtr.org /ISSN:1943-8141/AJTR0166623

Original Article

Role of the PSMC1 gene in the pathological progression of Parkinson's disease

Yaoyong Wang[1*], Yifan Li[2*], Zihan Chen[2], Yongchen Zhao[2]

[1]Medical School of Chinese PLA, Beijing 100853, China; [2]Department of Integrative Traditional Chinese and Western Medicine, Affiliated Hospital of Hebei University, Baoding 071000, Hebei, China. [*]Equal contributors and co-first authors.

Received June 6, 2025; Accepted October 29, 2025; Epub November 15, 2025; Published November 30, 2025

Abstract: Objective: To explore the association between Parkinson's disease (PD) and the expression of ubiquitin-related proteins, and to elucidate its potential significance. Methods: Differential expression analyses were performed using the GSE20141, GSE7621, and GSE20164 datasets to identify and intersect differentially expressed genes (DEGs). Functional enrichment analyses were conducted to further explore the biological significance of these DEGs. C57BL/6J mice were randomly divided into either a PD model group or a control group. Behavioral performance on the balance beam test and the expression levels of PSMC1, α-syn, UCH-1, and Parkin in the substantia nigra were compared between groups. Results: Gene overlap analysis across the three datasets identified 25 core DEGs, among which PSMC1 was the only ubiquitin-proteasome system (UPS)-related gene. Compared with the controls, the number of paw slips from balance beam in the model group significantly increased after 3, 6, and 10 modeling sessions ($P<0.05$). The mRNA expression levels of PSMC1, UCH-1, and Parkin in the substantia nigra of the model group mice significantly decreased ($P<0.05$), whereas the mRNA expression of α-syn significantly increased ($P<0.05$). Conclusions: Integrating bioinformatics with experimental verification, this study confirms that dysregulation of key UPS genes-particularly PSMC1-is closely related to the pathological process of PD.

Keywords: Parkinson's disease, ubiquitin-related protein, bioinformatics, expression meaning

Introduction

Parkinson's disease (PD), the second most prevalent neurodegenerative disorder, is characterized by progressive degeneration of dopaminergic neurons in the substantia nigra and the presence of Lewy bodies composed of aggregated α-synuclein [1, 2]. Accumulating evidence indicates that dysfunction of the ubiquitin-proteasome system (UPS) plays a critical role in PD pathogenesis, with aberrant expression of ubiquitin-related proteins emerging as a key molecular hallmark [3, 4]. As a central mechanism of cellular protein quality control, the UPS mediates the degradation of misfolded or damaged proteins through covalent ubiquitination and subsequent proteolysis by the 26S proteasome. Impairment of this pathway results in toxic protein accumulation, posing a direct threat to neuronal survival [5-7].

Numerous studies have demonstrated abnormal accumulation of ubiquitinated proteins in the brain of PD patients, and the colocalization of ubiquitin and α-synuclein within Lewy bodies suggests that defective UPS-mediated clearance may drive neurodegeneration [8-10]. Further genetic studies have found that PD-related genes, such as Parkin and UCH-L1 are involved in the regulation of ubiquitination, and their mutations can lead to the loss of E3 ubiquitin ligase activity or abnormal deubiquitination, thereby compromising UPS-mediated protein clearance [11-13]. Notably, altered expression of ubiquitin ligase hHrd1 in PD animal models implies its potential neuroprotective role in regulating misfolded protein ubiquitination [14, 15]. In addition, proteasome inhibition induced by environmental toxins has been shown to accelerate α-synuclein aggregation and dopaminergic neuron apoptosis, recapitulating the typical pathology of PD [16, 17].

https://doi.org/10.62347/BWYD6434

Although previous studies have provided initial insights into the role of UPS in PD, the dynamic expression patterns of ubiquitin-related proteins across different disease stages and the mechanisms by which their interaction networks maintain neuronal homeostasis remain poorly understood. For instance, the effects of specific ubiquitin chain modifications on substrate protein fate, compensatory activity of specific E3 ubiquitin ligases under cellular stress, and crosstalk between the UPS and other protein degradation pathways-such as autophagy-require further clarification. In this study, we systematically analyzed the association between PD and ubiquitin-related proteins using bioinformatics approaches, followed by experimental validation in an animal model.

Materials and methods

UPS gene set

A total of 854 genes related to the UPS were identified based on Gene Ontology (GO) Biological process (BP) annotation. The misgdbr package was used to extract genes containing the keyword "Ubiqutin" from the C5 (GO gene set) category of the Molecular Signatures Database (MSigDB). These genes are primarily involved in ubiquitination, protein degradation and related regulatory processes.

Dataset information

Transcriptomic datasets were obtained from the Gene Expression Omnibus (GEO) database (http://www.ncbi.nlm.nih.gov/geo/). Three brain tissue datasets (GSE20141, GSE7621, and GSE20164) were included in this study. GSE20141 comprised 18 samples (10 PD samples and 8 control samples), GSE7621 comprised 25 samples (16 PD and 9 control), and GSE20164 comprised 11 samples (6 PD and 5 control).

Analytical methods

Differential expression analysis was performed using the limma package, which applies linear modeling and bayesian statistics to effectively process gene expression microarray data. Differentially expressed genes (DEGs) were identified according the criteria $P<0.05$ and $|\log2FC|>1$. For each dataset, both genome-wide DEGs and DEGs associated with UPS were identified.

For probe-to-gene conversion, the maxmean method was used, in which the probe with the highest signal intensity was selected to represent the gene when multiple probes mapped to the same gene. In addition, principal component analysis (PCA) was performed to evaluate global expression pattern variations among samples, and Venn diagrams were generated to assess the overlap of DEGs across different datasets.

To further elucidate the biological significance of the identified DEGs, functional enrichment analyses, including Gene Ontology (GO) biological process enrichment and Kyoto Encyclopedia of Genes and Genomes (KEGG) pathway enrichment analyses, were performed.

Co-expression analysis of core genes and screening of targeted intervention agents

Co-expression analysis of core genes was conducted using the genemania database (https://genemania.org/search/homo-sapiens/). Additionally, potential targeted intervention genes were screened using the Enrichr platform (https://maayanlab.cloud/Enrichr/).

Experimental animals and grouping

Twelve-week-old SPF male C57BL/6J mice weighing 25-30 g were obtained from the model animal research institute of Nanjing university. All mice were housed under controlled environmental conditions with ad libitum access to food and water. The room temperature was maintained at about 22°C, relative humidity at about 50%, and a 12 h light/dark cycle was applied.

The mice were randomly divided into a model group and a control group, with 20 mice in each group. Mice in the model group were intraperitoneally injected of probenecid solution (100 mg/kg; Shanghai Aladdin Bio-Chem Technology Co., Ltd., China), followed by MPTP (25 mg/kg; Sigma, CAS: 23007-85-4) 30 min later. This regimen was administered once every 3.5 days for 10 consecutive injections. Control mice were intraperitoneally injected of an equal volume of normal saline following the same schedule and procedure.

Mouse balance beam test

A modified balance beam was used for behavioral test. The beam, made of acrylic material,

Table 1. Primer sequences

Primers	Sequence
PSMC1	Upstream primer: 5'-CACACTCAGTGCCGGTTAAAA-3'
	Downstream primer: 5'-GTAGACACGATGGCATGATTGT-3'
Alpha syn	Upstream primer: 5'-AAGAGGGTGTTCTCTATGTAGGC-3'
	Downstream primer: 5'-GCTCCTCCAACATTTGTCACTT-3'
UCH-1	Upstream primer: 5'-ATGAGGCAACATGATGTGCAG-3'
	Downstream primer: 5'-TGGTACAGACGATAGATGAGGTC-3'
Parkin	Upstream primer: 5'-AAATGCCCAGACAAGATGCC-3'
	Downstream primer: 5'-GGCCTCTCACGACTGAGTT-3'
GAPDH	Upstream primer: 5'-CTGGGCTACACTGAGCACC-3'
	Downstream primer: 5'-AAGTGGTCGTTGAGGGCAATG-3'

was 100 cm in length and 1.5 cm in thickness, with the width sequentially reduced from 3.5 cm to 2 cm, and then to 1 cm from the starting to the terminal end. A metal mesh (0.6 cm × 0.6 cm) was fitted over the beam surface to prevent slipping and to facilitate video recording of paw slips during traversal.

At the beginning of each experiment, mice were placed at the starting end of the beam facing their home cage, which was positioned at the opposite end to serve as a visual and olfactory incentive. Video recordings were used to capture instances of paw slips while crossing the beam. Prior to modeling, all mice were pretrained to traverse the beam five times per day for three consecutive days to ensure task familiarity and consistent performance.

During the formal experiment, balance beam tests were performed in both groups at baseline (0) and after 3, 6, and 10 modeling sessions. Each mouse was tested 5 times per session, with a minimal interval of 2 minutes between trials. Finally, the number of paw drops during traversal was counted, and the mean value was used to evaluate the motor balance and coordination of each mouse.

RT-qPCR detection

At four time points (0, 3, 6 and 10 modeling sessions), five mice were randomly selected from each group. The mice were anesthetized in an induction chamber with 4%-5% isoflurane and euthanized by cervical dislocation. The brain tissues were removed, and the midbrain was dissected to isolate the substantia nigra with fine forceps. The tissues were immediately frozen in liquid nitrogen and stored at -80°C until analysis. All procedures were approved by the Affiliated Hospital of Hebei University.

Total RNA was extracted using TRIzol reagent (Invitrogen, USA), and RNA concentration and purity were determined spectrophotometrically. Complementary DNA (cDNA) was synthesized from total RNA using a reverse transcription kit (Shanghai Biyuntian Biotechnology Co., LTD.). RT-qPCR was carried out under the following cycling conditions: 95°C for 6 min; 45 cycles of 95°C for 10 s, 60°C for 30 s, 72°C for 10 s; followed by a final step at 95°C for 15 s. Primer sequences are shown in **Table 1**. Relative gene expression levels were calculated using the $2^{-\Delta\Delta Ct}$ method. All primers were synthesized by Shanghai Sangon biotechnology Co., Ltd. (China).

Statistical analysis

All statistical analyses were performed using SPSS 27.0. Measurement data were expressed as mean ± standard deviation ($\bar{x}$ ± s). Differences between the two groups were analyzed using the t-tests. Repeated-measures analysis of variance (ANOVA) followed by LSD test was used for comparisons across different time points. Categorical variables were expressed as percentages and compared using the χ^2 test. A P value <0.05 was considered statistically significant.

Results

Differentially expressed genes

Differential expression analyses (**Figure 1**) identified 2,082 DEGs in the GSE20141 dataset, including 1,235 upregulated genes and 847 downregulated genes. In the GSE7621 dataset, 2,824 DEGs were identified, including 1,486 upregulated genes and 1,338 downregulated genes. The GSE20164 dataset revealed 1,005 DEGs, including 439 upregulated genes and 566 downregulated genes.

Changes in USP-related gene expression

Among the DEGs from each dataset, those associated with the USP were further analyzed.

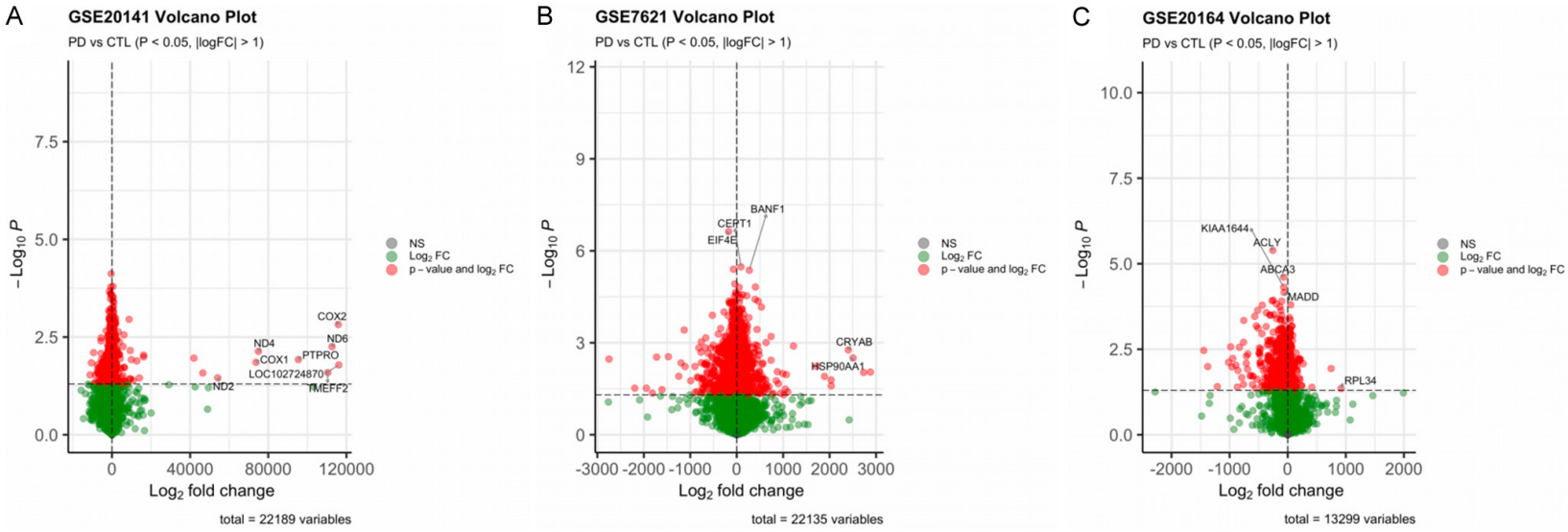

Figure 1. Volcano plot of differential gene expression in each dataset. A: Volcano plot of DEGs in GSE20141; B: Volcano map of DEGs in GSE7621; C: Volcano map of DEGs in GSE20164. DEG: differentially expressed gene.

The GSE20141 dataset contained 103 UPS-related DEGs, the GSE7621 dataset contained 121, and the GSE20164 dataset contained 47 (**Figure 2**).

Principal component and gene overlap analyses

Principal component analysis (PCA) revealed partial separation between the control group and PD group in the first principal component (Dim) in all three datasets (GSE20141, GSE7621 and GSE20164). Venn diagram analysis of overlapping DEGs identified 25 core genes shared among the three datasets, with PSMC1 being the only UPS-related gene (**Figure 3**).

Functional enrichment analysis

GO enrichment analysis showed that pathways closely related to PD were mainly involved in mitochondrial oxidative respiration, synaptic vesicle transport/neuronal signaling, RNA processing, and hormone-related processes. KEEG pathway analysis indicated enrichment in mitochondrial protein degradation networks, synaptic vesicle recycling, and lysosomal/autophagy-associated degradation pathways (**Figure 4**).

Co-expression analysis based on core genes

As shown in **Figure 5**, the core gene PSMC1 was co-expressed with 20 other genes. The interactions among these genes were primarily involved in biological processes such as mitochondrion localization, microtubule-mediated mitochondrion transport, organelle trafficking along microtubules, and vesicular transport.

GO and KEGG analysis of core genes

GO and KEGG enrichment analyses of the core genes demonstrated that the Type I diabetes mellitus and basal transcription factor pathways were among the top enriched pathways (**Figure 6A**). GO analysis further indicated that these core genes were mainly involved in biological processes such as organelle membranes, response to hypoxia, and adaptation to decreased oxygen levels (**Figure 6B**).

Screening of targeted therapeutic agents

Using the Enrichr platform, five potential targeted therapeutic agents were identified. These compounds may modulate PD progression by interfering with the above-mentioned molecular pathways (**Table 2**).

Behavioral results of the balance beam

At baseline (0 modeling sessions), there was no significant difference in the number of paw slips between the two groups *(P>0.05)*. With an increasing number of modeling sessions, paw slip frequency in the model group also gradually increased. Compared with the control group, the number of paw slips after 3, 6 and 10 modeling sessions was significantly increased in the model group ($P<0.05$) (**Figure 7**).

Comparison of gene expression between groups

With the increase of modeling sessions, the relative mRNA expression levels of PSMC1, UCH-1, and Parkin in the substantia nigra of model mice were significantly decreased ($P<0.05$), whereas the relative expression level of α-syn mRNA was significantly increased ($P<0.05$) (**Figure 8**).

Discussion

As the second most prevalent neurodegenerative disorder worldwide, PD has drawn significant attention regarding the contribution of UPS dysfunction to its pathogenesis. Recent studies have demonstrated that mutations in genes encoding key UPS components-such as Parkin and UCH-L1-can lead to the accumulation of misfolded proteins and trigger dopaminergic neuron apoptosis [18-21]. Emerging evidence suggests that gut bacteriophages may influence UPS activity through the microbiota-gut-brain axis, revealing novel interactions between environmental and genetic factors in PD development [22, 23]. In this study, bioinformatics analysis combined with experimental validation confirmed the close association between UPS dysregulation and PD progression.

Animal experiments demonstrated that the mRNA expression of PSMC1, UCH-L1, and Parkin was significantly down-regulated, whereas α-syn expression was significantly up-regulated in MPTP-induced PD model mice, consistent with the transcriptomic profiles of human PD brain tissues [24, 25]. As a regulatory subunit of the 26S proteasome, reduced PSMC1

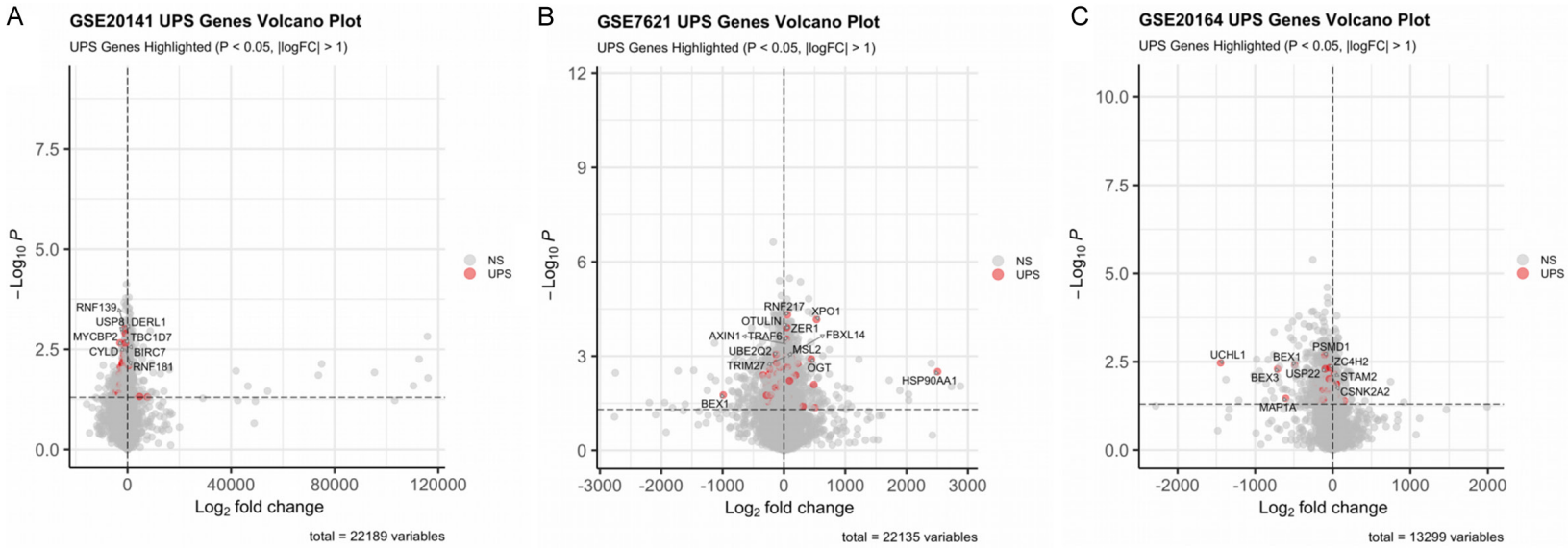

Figure 2. Volcano plot of USP-related differentially expressed genes in three datasets. A: Volcano plot of USP-related DEGs in GSE20141 dataset; B: Volcano plot of USP-related DEGs in GSE7621 dataset; C. Volcano plot of USP-related DEGs in GSE20164 dataset. Note: DEG: differentially expressed gene; UPS: ubiquitin-proteasome system.

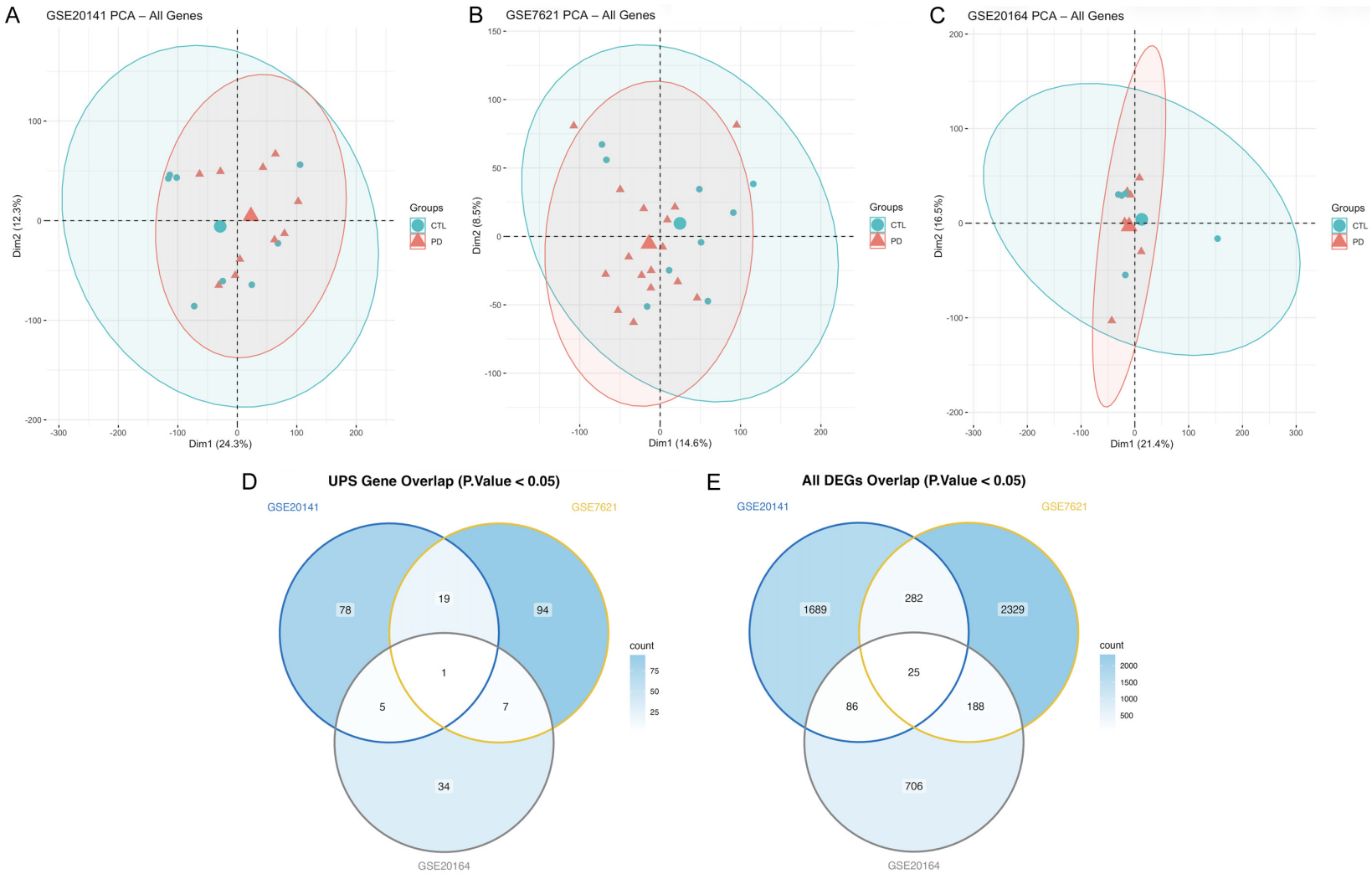

Figure 3. Principal component analysis plot and gene overlap analysis plot. A: PCA Plot of GSE20141 dataset; B: PCA Plot of GSE7621 dataset; C: PCA Plot of GSE20164 dataset; D: Overlap of UPS-related DEGs across the three datasets; E: Overlap of all DEGs across the three datasets. Note: PCA: principal component analysis; DEG: differentially expressed gene; UPS: ubiquitin-proteasome system.

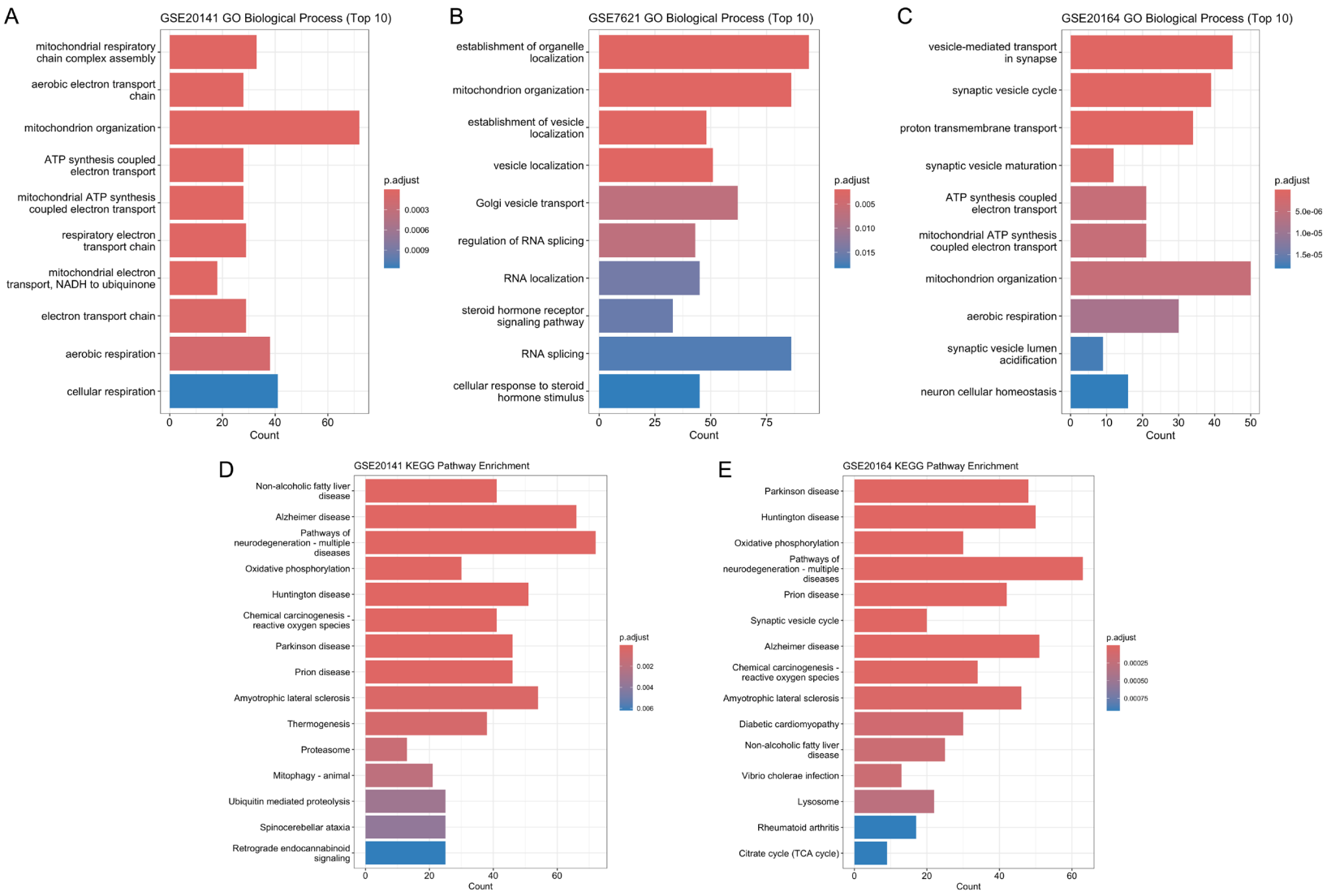

Figure 4. Functional enrichment analysis. A: GO biological process enrichment analysis for the GSE20141 dataset; B: GO biological process enrichment analysis for the GSE7621 dataset; C: GO biological process enrichment analysis for the GSE20164 dataset; D: KEGG pathway enrichment analysis for the GSE20141 dataset; E: KEGG pathway enrichment analysis for the GSE20164 dataset. Note: GO: Gene Ontology; KEGG: Kyoto encyclopedia of genes and genomes.

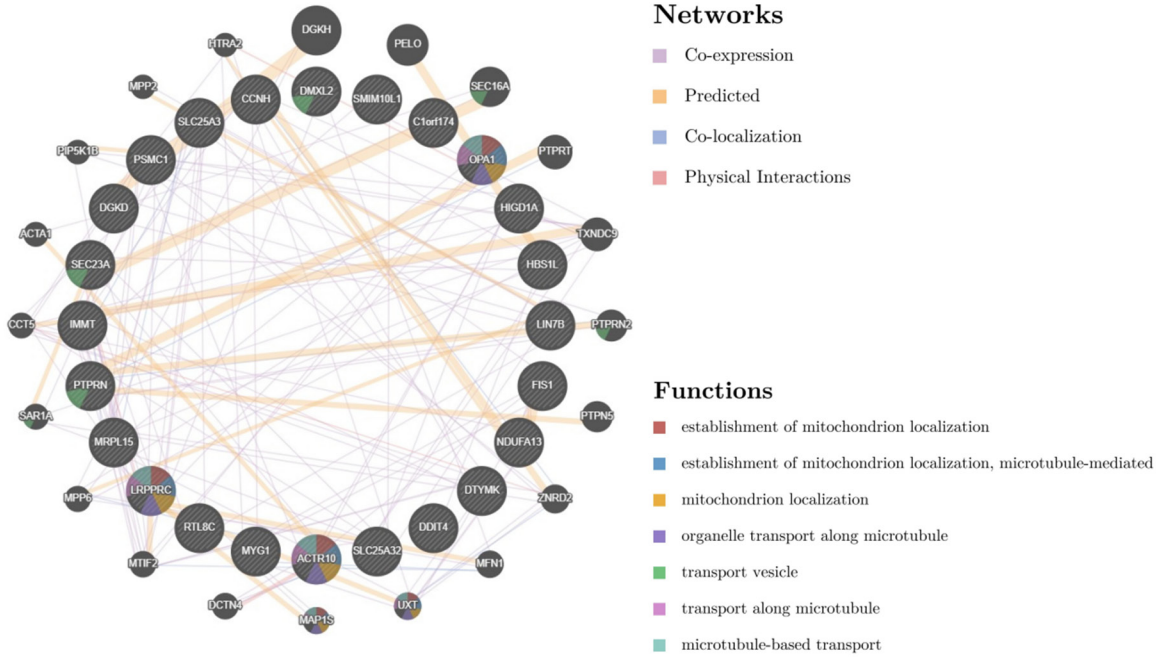

Figure 5. Co-expression analysis of core genes.

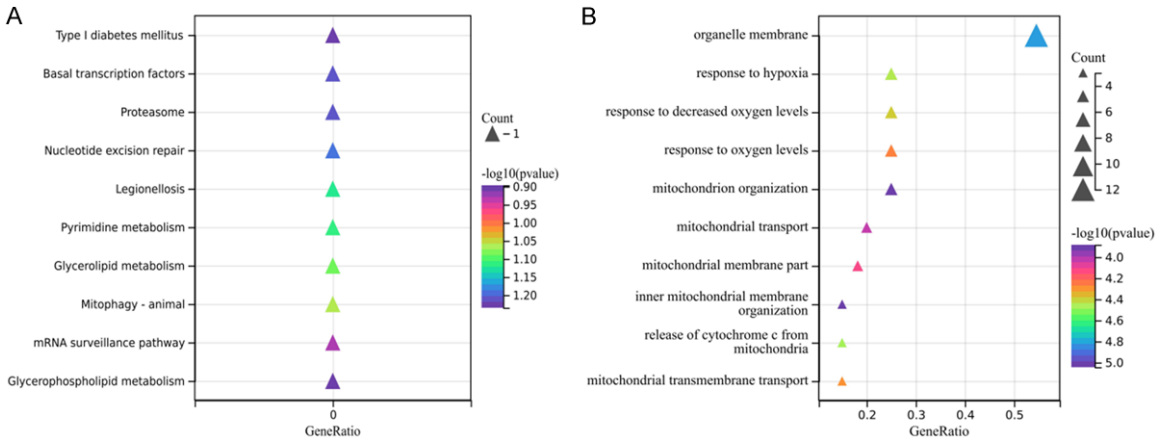

Figure 6. Functional enrichment analysis of core genes. A: KEGG Pathway Enrichment; B: GO Biological Process Enrichment. Notes: GO: Gene Ontology; KEGG: Kyoto encyclopedia of genes and genomes.

Table 2. Top-ranked targeted interventions

Term	*P*-value	Adjusted *P*-value	Combined Score
Elesclomol	0.0025	0.0128	119530
QUINOLINE	0.0032	0.0128	114525
5, 6-BENZOFLAVONE	0.009	0.0184	93135
Copper (II) chloride	0.0092	0.0184	92909
(17S)-17-hydroxy-13,17-dimethyl-1,2,6,7,8,14,15,16-octahydrocyclopenta[a]phenanthren-3-one	0.0183	0.0294	78495

expression may compromise proteasomal degradation of misfolded or damaged proteins. Meanwhile, downregulation of UCH-L1 (a deubiquitinating enzyme) and Parkin (an E3 ubiqui-

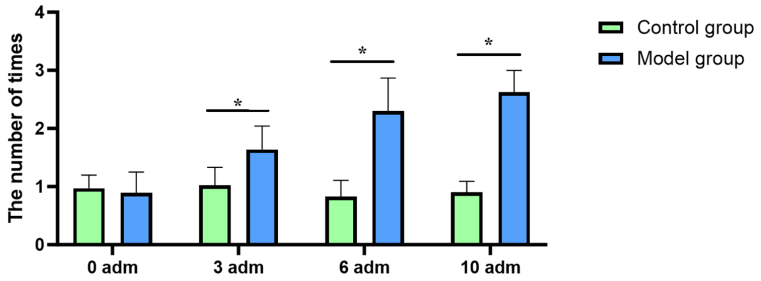

Figure 7. Behavioral test results. Note: *P<0.05.

tin ligase) further exacerbates the accumulation of ubiquitinated proteins [26, 27]. Notably, overexpression of α-syn promotes oligomerization, which not only directly inhibits proteasome catalytic activity but also perpetuates UPS dysfunction through a self-reinforcing feedback loop [28, 29]. Correspondingly, behavioral assessments revealed progressive deterioration of balance performance in PD model mice with increasing numbers of modeling sessions, indicating a temporal correlation between motor deficits and altered UPS-related gene expression. Collectively, these findings support a pathogenic cascade involving UPS impairment, α-syn aggregation, and subsequent dopaminergic neuronal loss.

The study revealed the dynamic changes of key components of the UPS in a PD model. By integrating transcriptome analysis of three independent datasets (GSE20141, GSE7621 and GSE20164), PSMC1 was identified as the only UPS core gene consistently downregulated across all datasets. PSMC1 encodes the ATPase subunit of the 26S proteasome, and its reduced expression may lead to proteasome assembly defects. Recent cryo-electron microscopy studies have shown that conformational change in PSMC1 directly affects substrate unfolding efficiency; a 30% reduction in PSMC1 expression decreases the chymotrypsin-like activity of the β5 subunit by approximately 42% [30, 31]. This explains the molecular basis of abnormal protein aggregation observed in the brains of PD model mice.

In behavioral tests, the motor coordination of the model group deteriorated with an increase in the modeling frequency, confirming the temporal correlation between motor dysfunction and UPS-related gene dysregulation, findings consistent with previous reports [32]. These findings support the "UPS functional collapse-α-syn aggregation-neuronal damage" cascade hypothesis [33].

This study, through the combination of bioinformatics and animal experiments, revealed the potential importance of PSMC1 in PD pathogenesis. However, as only three publicly available human brain transcriptome datasets were analyzed, the sample size and source diversity were relatively limited. Therefore, the findings may not fully represent the overall genetic variability and disease heterogeneity present in the broader PD population. At the same time, although PSMC1 downregulation was confirmed in PD mice, its upstream regulators and downstream effectors remain to be elucidated. Further research is warranted to clarify the specific regulatory mechanism of PSMC1 in PD.

Conclusion

Dysregulation of UPS key genes, especially PSMC1, is closely associated with PD progression. PSMC1 may serve as a pivotal molecule linking genetic factors (e.g., Parkin mutations) with environmental toxins, such as MPTP exposure. Future research should focus on: (1) developing small-molecule modulators targeting PSMC1; (2) investigating deubiquitinizing enzymes (DUBs) capable of degrading α-syn aggregates; and (3) integrating serum proteomics to identify early diagnostic markers. Collectively, these findings provide novel insights into PD pathogenesis and lay a theoretical foundation for precision treatment strategies targeting UPS regulation.

Acknowledgements

This research was supported by Hebei Provincial Major Medical Research Funding Project (No. 2013067759).

Disclosure of conflict of interest

None.

Address correspondence to: Yongchen Zhao, Department of Integrative Traditional Chinese and Western Medicine, Affiliated Hospital of Hebei

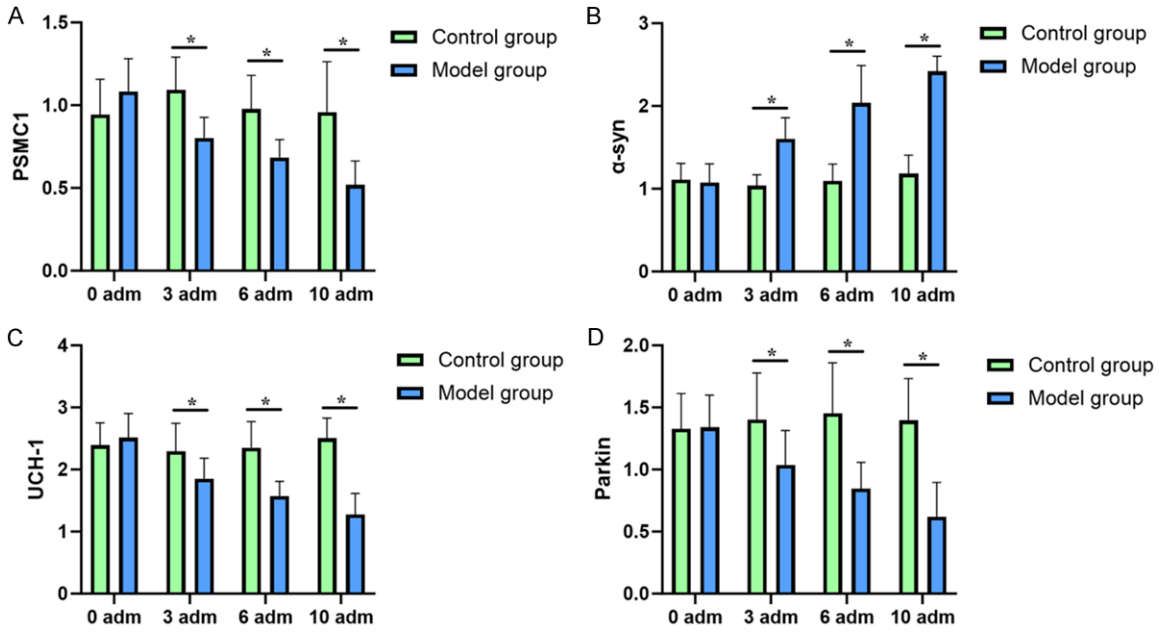

Figure 8. Comparison of related gene expression between the two groups of mice. A: mRNA expression of PSMC1; B: mRNA expression of α-syn; C: mRNA expression of UCH-1; D: mRNA expression of Parkin. *P<0.05.

University, No. 212 Yuhua East Road, Baoding 071000, Hebei, China. Tel: +86-0312-5981818; E-mail: zhaoyongchen69@163.com

References

[1] Cattaneo C and Jost WH. Pain in Parkinson's disease: pathophysiology, classification and treatment. J Integr Neurosci 2023; 22: 132.

[2] Weintraub D, Aarsland D, Chaudhuri KR, Dobkin RD, Leentjens AF, Rodriguez-Violante M and Schrag A. The neuropsychiatry of Parkinson's disease: advances and challenges. Lancet Neurol 2022; 21: 89-102.

[3] Pajares M, I Rojo A, Manda G, Bosca L and Cuadrado A. Inflammation in Parkinson's disease: mechanisms and therapeutic implications. Cells 2020; 9: 1687.

[4] Rajan S and Kaas B. Parkinson's disease: risk factor modification and prevention. Semin Neurol 2022; 42: 626-638.

[5] Day JO and Mullin S. The genetics of Parkinson's disease and implications for clinical practice. Genes (Basel) 2021; 12: 1006.

[6] Borsche M, Pereira SL, Klein C and Grunewald A. Mitochondria and Parkinson's disease: clinical, molecular, and translational aspects. J Parkinsons Dis 2021; 11: 45-60.

[7] Vrijsen S, Houdou M, Cascalho A, Eggermont J and Vangheluwe P. Polyamines in Parkinson's disease: balancing between neurotoxicity and neuroprotection. Annu Rev Biochem 2023; 92: 435-464.

[8] Horsager J and Borghammer P. Brain-first vs. body-first Parkinson's disease: an update on recent evidence. Parkinsonism Relat Disord 2024; 122: 106101.

[9] Dovonou A, Bolduc C, Soto Linan V, Gora C, Peralta Iii MR and Levesque M. Animal models of Parkinson's disease: bridging the gap between disease hallmarks and research questions. Transl Neurodegener 2023; 12: 36.

[10] Chen R, Gu X and Wang X. Alpha-Synuclein in Parkinson's disease and advances in detection. Clin Chim Acta 2022; 529: 76-86.

[11] Schalkamp AK, Peall KJ, Harrison NA and Sandor C. Wearable movement-tracking data identify Parkinson's disease years before clinical diagnosis. Nat Med 2023; 29: 2048-2056.

[12] Mele B, Van S, Holroyd-Leduc J, Ismail Z, Pringsheim T and Goodarzi Z. Diagnosis, treatment and management of apathy in Parkinson's disease: a scoping review. BMJ Open 2020; 10: e037632.

[13] Hill DR, Huters AD, Towne TB, Reddy RE, Fogle JL, Voight EA and Kym PR. Parkinson's disease: advances in treatment and the syntheses of various classes of pharmaceutical drug substances. Chem Rev 2023; 123: 13693-13712.

[14] Vaidya B, Dhamija K, Guru P and Sharma SS. Parkinson's disease in women: mechanisms physicist sex differences. Eur J Pharmacol 2021; 895: 173862.

[15] Ahmad MH, Rizvi MA, Ali M and Mondal AC. Neurobiology of depression in Parkinson's dis-

ease: insights into epidemiology, molecular mechanisms and treatment strategies. Ageing Res Rev 2023; 85: 101840.
[16] Polissidis A, Petropoulou-Vathi L, Nakos-Bimpos M and Rideout HJ. The future of targeted gene-based treatment strategies and biomarkers in Parkinson's disease. Biomolecules 2020; 10: 912.
[17] Kalyanaraman B, Cheng G and Hardy M. Gut microbiome, short-chain fatty acids, alpha-synuclein, neuroinflammation, and ROS/RNS: relevance to Parkinson's disease and therapeutic implications. Redox Biol 2024; 71: 103092.
[18] Varesi A, Campagnoli LIM, Fahmideh F, Pierella E, Romeo M, Ricevuti G, Nicoletta M, Chirumbolo S and Pascale A. The interplay between gut microbiota and Parkinson's disease: implications on diagnosis and treatment. Int J Mol Sci 2022; 23: 12289.
[19] Robea MA, Balmus IM, Ciobica A, Strungaru S, Plavan G, Gorgan LD, Savuca A and Nicoara M. Parkinson's disease-induced zebrafish models: focussing on oxidative stress implications and sleep processes. Oxid Med Cell Longev 2020; 2020: 1370837.
[20] Kumar S, Goyal L and Singh S. Tremor and rigidity in patients with Parkinson's disease: emphasis on epidemiology, pathophysiology and contributing factors. CNS Neurol Disord Drug Targets 2022; 21: 596-609.
[21] Vizziello M, Borellini L, Franco G and Ardolino G. Disruption of mitochondrial homeostasis: the role of PINK1 in Parkinson's disease. Cells 2021; 10: 3022.
[22] Ma L, Li X, Liu C, Yan W, Ma J, Petersen RB, Peng A and Huang K. Modelling Parkinson's disease in C. elegans: strengths and limitations. Curr Pharm Des 2022; 28: 3033-3048.
[23] Liu WY, Tung TH, Zhang C and Shi L. Systematic review for the prevention and management of falls and fear of falling in patients with Parkinson's disease. Brain Behav 2022; 12: e2690.
[24] Prasuhn J and Bruggemann N. Genotype-driven therapeutic developments in Parkinson's disease. Mol Med 2021; 27: 42.
[25] Lintel H, Corpuz T, Paracha SU and Grossberg GT. Mood disorders and anxiety in Parkinson's disease: current concepts. J Geriatr Psychiatry Neurol 2021; 34: 280-288.
[26] Zhao B, Cheung R and Malvankar-Mehta MS. Risk of Parkinson's disease in glaucoma patients: a systematic review and meta-analysis. Curr Med Res Opin 2022; 38: 955-962.
[27] Xiong Y and Yu J. LRRK2 in Parkinson's disease: upstream regulation and therapeutic targeting. Trends Mol Med 2024; 30: 982-996.
[28] Deng X, Mehta A, Xiao B, Ray Chaudhuri K, Tan EK and Tan LC. Parkinson's disease subtypes: approaches and clinical implications. Parkinsonism Relat Disord 2025;130:107208.
[29] Zhang PF and Gao F. Neuroinflammation in Parkinson's disease: a meta-analysis of PET imaging studies. J Neurol 2022; 269: 2304-2314.
[30] Ebina J, Ebihara S and Kano O. Similarities, differences and overlaps between frailty and Parkinson's disease. Geriatr Gerontol Int 2022; 22: 259-270.
[31] Berg D, Bloem BR, Kalia LV and Postuma RB. Introduction: the earliest phase of Parkinson's disease: possibilities for detection and intervention. J Parkinsons Dis 2024; 14: S253-S255.
[32] Guerra A, D'Onofrio V, Ferreri F, Bologna M and Antonini A. Objective measurement versus clinician-based assessment for Parkinson's disease. Expert Rev Neurother 2023; 23: 689-702.
[33] Arango D, Bittar A, Esmeral NP, Ocasion C, Munoz-Camargo C, Cruz JC, Reyes LH and Bloch NI. Understanding the potential of genome editing in Parkinson's disease. Int J Mol Sci 2021; 22: 9241.